

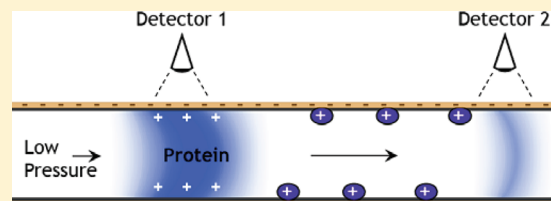
# Pressure-Based Approach for the Analysis of Protein Adsorption in Capillary Electrophoresis

Stephanie de Jong and Sergey N. Krylov\*

Department of Chemistry and Centre for Research on Biomolecular Interactions, York University, Toronto, Ontario M3J 1P3, Canada

Supporting Information

**ABSTRACT:** Protein adsorption to inner capillary walls creates a major obstacle in all applications of capillary electrophoresis involving protein samples. The problem is especially severe in kinetic capillary electrophoresis (KCE) techniques, which are used to study protein–ligand interactions at physiological conditions and, thus, cannot utilize extreme pH. A variety of coatings exist to reduce protein adsorption in CE, each expressing a unique surface chemistry that interacts with individual proteins differently. Here we introduce a simple pressure-based method for the qualitative assessment of protein adsorption that can facilitate the direct antiadhesive ranking of several coatings toward a protein of interest. In this approach, a short plug of the protein is injected into a capillary and propagated through with a pressure low enough to ensure adequate Taylor dispersion. The experiment is performed with a nonmodified commercial instrument in a pseudo-two-detector approach. The two detectors are mimicked by using two different distances from the capillary inlet to a single detector. If the peak area and shape do not change with changing distance, the protein does not adsorb appreciably, while a decreasing peak area with increasing distance infers inner surface adsorption. The magnitude change of the peak area between the two distances along with the overall peak shape is used to gauge the extent of protein adsorption. By using this method, we ranked antiadhesive properties of different wall chemistries for a series of proteins. The described method will be useful for optimizing protein analysis by CE and, in particular, for KCE experiments that investigate how proteins interact with their respective ligands.



Kinetic capillary electrophoresis (KCE) is a conceptual platform comprised of several CE-based affinity methods that can comprehensively characterize binding affinity between two molecules that interact during separation.<sup>1</sup> The well-controlled partitioning capabilities of CE combined with the ability to elucidate kinetic and equilibrium constants ( $k_{on}$ ,  $k_{off}$  and  $K_d$ ) makes KCE methods ideal for investigating biomolecular interactions.<sup>2–8</sup> Protein–ligand interactions are one of the most compelling to study as they govern a vast array of important cellular processes. Unfortunately, the undisturbed migration of proteins in CE and, hence, any corresponding protein–ligand complexes is often hindered by their adsorption to the inner surface of the fused-silica capillary.<sup>9–11</sup>

At physiological pH, the silanol groups of the inner capillary surface retain a considerable negative charge (average  $pK(\text{SiOH}) = 6.3$ ).<sup>12</sup> Being amphiphilic molecules, many proteins have locally contained regions of net positive charge that experience electrostatic attraction to the capillary surface. This multisite protein–capillary interaction obscures the CE separation of free ligand from the protein–ligand complex, which complicates their analysis by KCE. Protein adsorption also creates a challenge in KCE-based aptamer selection and, depending on the protein affinity for the surface, may completely inhibit the selection of aptamers for therapeutically important targets. Therefore, protein adsorption must be eliminated prior to the KCE analysis of the equilibrium mixture, which contains both the protein and ligand components.

One approach to reduce the surface interaction is to adjust the pH of the background electrolyte to either extremely acidic or extremely basic conditions. Low-pH buffers significantly reduce the charge of the inner capillary surface and effectively eliminate any electrostatic attraction that would otherwise occur with the protein sample.<sup>13</sup> Alternatively, increasing the pH to a value above the protein's isoelectric point promotes the Coulombic repulsion between the protein and negatively charged capillary.<sup>14</sup> Although this presents a relatively simple solution, protein–ligand interactions are highly pH sensitive and physiological conditions are necessary to ensure proper protein structure as well as suitable ligand binding.

A more practical approach used to prevent the adsorption of basic proteins is to mask the highly dense negative surface charge with dynamic modifiers or permanently bound coatings. Since the adsorption of proteins is generally a cooperative process, a reduction in the surface charge should yield an exponential decrease in the strength of protein–capillary interactions.<sup>15,16</sup> When analyzing basic proteins in CE, a common approach is to completely reverse the surface charge of the capillary through the use of cationic chemical additives or coatings.<sup>17–21</sup> However, charge reversal becomes problematic in KCE analysis of protein–ligand

Received: November 15, 2011

Accepted: November 22, 2011

Published: November 22, 2011

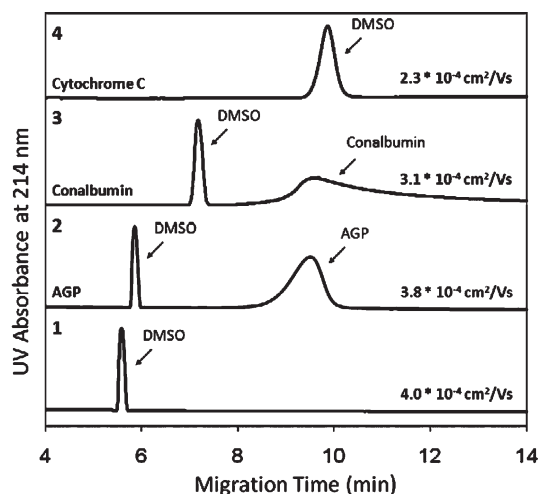


**Figure 1.** UV absorbance data demonstrating how protein adsorption influences the EOF in an untreated fused-silica capillary. CE separation was performed at 300 V/cm using a 50 mM Tris acetate (pH 8.2) run buffer. In each trace, 0.2% DMSO was used as a neutral EOF marker. Trace 1 presents DMSO migration in the absence of any protein. The calculated EOF mobilities are shown on the right. Traces 2–4 present results where protein samples of varying adsorptive properties are introduced into the capillary. AGP was selected as an example of nonadsorptive protein (2), conalbumin as a moderately adsorptive representative (3), and cytochrome *c* as a highly adsorptive protein (4). All proteins were diluted to the same final concentration of 4 mg/mL and injected into the uncoated capillary together with DMSO. For cytochrome *c*, no protein peak is visible due to irreversible adsorption at the inner capillary surface and the limited detection capabilities of UV absorbance.

interactions if the ligand is negatively charged at neutral pH. This is exactly the case with DNA (or RNA) aptamers, which experience a strong electrostatic attraction to positively charged capillary surfaces. Both proteins and ligands vary in their physical-chemical properties, and each component will demonstrate a unique interaction with a surface coating at the molecular level. As a result, there is no simple and universal solution to prevent analyte adsorption that is compatible with KCE studies on biomolecular interactions. Many proteins of therapeutic and diagnostic importance tend to adsorb to the inner capillary surface, which then prevents both the KCE analysis and KCE-based aptamer selection until the proper coating or buffer additive is selected.

Selecting the appropriate coating requires a direct comparison of their antiadhesive properties toward the protein (and ligand) of interest. Generally, in CE, the extent of adsorption is monitored indirectly by assessing the separation efficiency during electrophoresis.<sup>22</sup> This approach is unreliable when it comes to ranking capillary coating effectiveness. Many factors influence a protein's electrophoretic migration pattern, the most notable being buffer conductivity and the capillary surface charge. Both of these elements may be altered with the use of dynamic or covalent modifiers and lead to peak broadening and reduction of the electroosmotic flow (EOF) even without the added complication of protein adsorption. Proteins themselves have also been shown to alter both the EOF and peak width due to high-affinity interactions with the capillary surface (see examples in Figure 1). Hence, electromigration is not a reliable approach when it comes to screening a series of coatings and buffer additives.

Righetti and co-workers suggested a method that detects irreversible protein adsorption by (i) saturating the capillary walls with the proteins, (ii) washing the capillary with a run buffer to remove the reversibly bound protein, and (iii) finally washing the capillary with a surfactant to displace the irreversibly bound proteins.<sup>23</sup> While being useful for other applications, this method does not assess the reversible binding, which is as important for KCE applications as irreversible binding, as it can equally affect the accuracy of KCE-based measurements.

The above-described difficulties motivated us to develop a simple pressure-based approach for the accurate characterization of protein adsorption. Conceptually, a short plug containing the protein solution is injected into the capillary and carried to the detector by applying a low pressure. The temporal propagation pattern is then analyzed by comparing the peak area and symmetry to those of a nonadsorptive control. To accurately characterize the degree of protein adsorption, we combined this pressure-based propagation technique with a dual-detection approach, first described by Towns and Regnier.<sup>11</sup> Although the original method uses a modified instrument with two on-capillary detectors, we employed a pseudo-dual-detection approach, later adapted by Tran et al.,<sup>24</sup> which does not require the use of a customized instrument.

While the concept of two detection points on a single capillary is well-established, it has always been coupled with electromigration to monitor the progress of sample adsorption. Using pressure-driven sample propagation, rather than electrophoresis, immediately eliminates any complications that may arise from variations in EOF introduced by the coating or additive itself. This simple independence of EOF allows us to draw conclusions directly on the coating's ability to prevent protein adsorption.

By comparing the change in peak areas and shapes at each detection point, we can qualitatively assess the coating's antiadhesive properties for the protein and ligand of interest. The method can be enhanced if the proteins are fluorescently labeled with Chromeo P503 pyrylium dye, which will improve the detection sensitivity.<sup>25,26</sup> Chromeo P503 does not alter the protein's charge upon labeling and should maintain the intrinsic protein–capillary interaction of the native protein.<sup>27</sup> Fluorescent labeling of the proteins enables the use of a lower protein concentration, which can more effectively define the protein's surface affinity.

## RESULTS AND DISCUSSION

If the pattern of pressure-driven protein propagation across a capillary is used to rank the coating efficiency, the applied pressure itself should not significantly influence its peak shape and symmetry. When a uniform forward pressure is introduced along the capillary cross-section, a parabolic laminar flow profile is produced with each injected plug. If the applied pressure is relatively high, the extent of transverse diffusion along the sample interface, with respect to the longitudinal propagation, is minimal and the sample will retain a parabolic shape as it reaches the detector.<sup>28</sup> This parabolic profile will distort the peak shape of the protein and is undesirable given that the migration pattern is used to assess protein adsorption. This peak deformation can be reduced to an insignificant level if the buffer velocity is slow enough to maximize the Taylor dispersion during the migration time between the initial and final (at the detector) positions of the plug (Figure 2). The amount of convection–diffusion obtained within the sample plug can be quantified in terms of its Péclet number,  $Pe$ . Provided that the analyte displays negligible adsorption to the

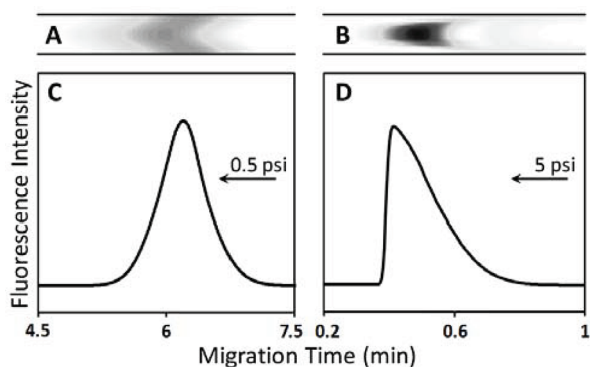


**Figure 2.** Pressure-driven migration profiles of the 100 nM thrombin-binding aptamer by applying either a low or high forward pressure. Sample plug schematics were created by using COMSOL Multiphysics modeling. The resulting parabolic pressure profiles were generated for pressures of 0.5 (A) and 5 (B) psi. Experimental electropherograms (C, D) are shown below the corresponding schematic representations. Tris acetate (50 mM, pH 8.2) was used as the run buffer, and the fluorescent emission was detected at 520 nm.

capillary, Péclet values of

$$Pe \equiv \frac{rv}{D} \ll \frac{L_d}{r} \quad (1)$$

will imply almost complete diffusion. Here,  $D$  is the diffusion coefficient,  $r$  is the capillary radius,  $v$  is the average velocity, and  $L_d$  is the distance from the injection end of the capillary to the detector. To assess how the applied pressure is correlated with the plug diffusivity, we chose a representative biomolecule (a thrombin-binding DNA aptamer) which had expressed a negligible affinity toward the surface of untreated fused-silica capillaries in the chosen run buffer. This allowed us to attribute any peak asymmetries to inadequate sample diffusion during the analysis time. By reducing the pressure, and corresponding flow rate, the detection time increases and allows for more effective diffusion. For the thrombin-binding aptamer, the pressure-induced migration pattern was measured using a range of separation pressures to establish an optimal pressure value that guarantees adequate sample diffusion (representative results are shown in Figure 2). It was found that, at a pressure of 0.5 psi, the DNA peaks appeared to be consistently symmetrical, and therefore, subsequent pressure propagation experiments were performed at this pressure.

To semiquantify the irreversible protein adsorption at the capillary surface, we adapted a simplified variation of the two-detector approach described by Tran et al.<sup>24</sup> This technique can accurately estimate the amount of irreversible protein adsorption by performing two experiments using the same sample and capillary. First, the sample is injected from the capillary inlet and carried toward the detector using a low forward pressure. In the second experiment, the sample is injected from the capillary outlet and then travels to the detection window by applying a pressure of the same magnitude but reverse direction. In the commercial instrument used in this study, the detection window is located in a fixed position of approximately 10 cm from the outlet end. However, the total distance from the inlet to the detector can be varied and is generally dependent on the experimental goals. In KCE-based methods, such as aptamer screening, the total length of the capillary is typically  $\sim 50$  cm, leaving a 40 cm propagation distance to the detection point. By integrating

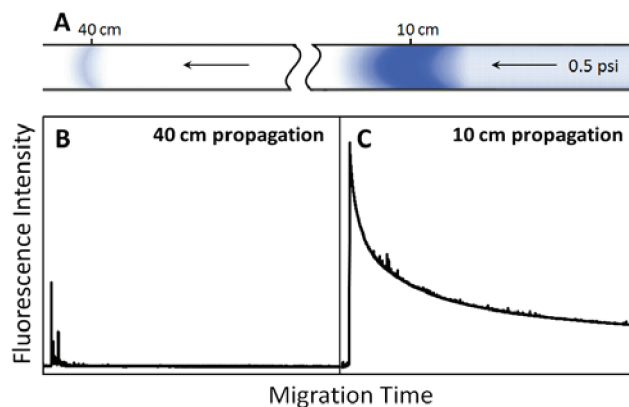


**Figure 3.** (A) Schematic representation of extensive protein adsorption which may occur within the capillary and how a reduction in sample concentration can be analyzed by using the two-detector pressure-driven approach. Panels B and C show the experimental migration pattern obtained from 40 and 10 cm propagation of 274  $\mu$ M Chromeo-labeled lysozyme, respectively. Protein fluorescence was detected at 610 nm using a 50 mM Tris acetate (pH 8.2) run buffer.

the peak area obtained at each distance (10 and 40 cm), the amount of protein adsorbed during a 30 cm propagation across the capillary can be calculated. Figure 3 illustrates a significant reduction in peak area, which suggests that the sample plug has been depleted due to strong irreversible interactions that the protein likely experiences at the surface. Often the peak shape itself provides some insight into the extent of protein adsorption. Proteins that demonstrate high surface adsorption typically produce a wide pressure-driven propagation profile with a substantial amount of tailing that occasionally coincides with a stepwise increase from the baseline. Therefore, the analysis of the temporal propagation pattern may also be used to assess the degree of reversible protein adsorption.

To demonstrate the applicability of this technique, we tested five proteins, each expressing different physical and chemical surface properties ( $\alpha_1$  acid glycoprotein (AGP), conalbumin, cytochrome  $c$ , thrombin, and lysozyme). Each protein was first injected into an uncoated capillary using the dual-detection, pressure-driven propagation method. It was determined that conalbumin, cytochrome  $c$ , thrombin, and lysozyme all experienced a high level of capillary adsorption. The protein–capillary interaction for lysozyme, thrombin, and cytochrome  $c$  was especially severe as they exhibited complete analyte loss during the 40 cm propagation, and the 10 cm propagations resulted in extremely broad peaks of negligible or low intensity (see Figures S1–S4 in the Supporting Information).

We then evaluated the antiadhesive properties of three coatings, two permanent and one dynamic, toward each of the five model proteins. Dynamic coatings are relatively easy to implement as they consist of simple additives which slightly modify the chemical composition of the background electrolyte. Dynamic additives range from ionic/nonionic surfactants to polymers and amine-containing molecules, each of which reversibly adsorbs to the negatively charged silanols of the capillary inner surface. Since the attachment is based on temporary interactions with the capillary surface, the agent present at a sufficiently high concentration tends to out-compete the protein for the available surface binding sites.<sup>29</sup> The dynamic coating used in this study, CELixir, is a commercially available, double-layer coating system which is

**Table 1. Antiadhesive Ranking of Capillary Surface Chemistries with Respect to Individual Protein Samples**

protein	SiOH	CElixir	PVA	LPA
AGP	1	1	2	2
conalbumin	3	1	1	2
cytochrome <i>c</i>	4	1	2	3
lysozyme	4	2	1	3
thrombin	4	2	1	3

offered in a range of pH values. The coating is applied by first rinsing the bare capillary with a polycationic initiator solution to form a stable positively charged surface. A second layer is then introduced by rinsing the capillary with a solution containing a buffered polyanion at the selected pH.

CElixir was originally developed as a means of achieving a stable and reproducible EOF, independent of the buffer pH. This fixed EOF is obtained by adjusting the negative charge density along the capillary surface to compensate for the variation in EOF that typically results from changes in pH.<sup>30,31</sup> For KCE methods, physiological pH is required to maintain the protein's native conformation, and for this purpose, a pH of 8.2 was selected.

We found that CElixir helped in suppressing the level of protein adsorbed for all five proteins tested. Although this dynamic modifier resulted in a major improvement compared to the bare silica, it was not an infallible means of preventing adsorption as each protein had demonstrated its own unique response to the coating. In particular, lysozyme had shown a significant tailing and a substantial loss of the protein sample between the 10 and 40 cm propagations (see Figures S1–S5 in the Supporting Information). This persistent adsorption is likely attributed to protein interaction with the anionic polymer that is temporarily retained on the capillary surface.

Permanent coatings, based on covalently or physically bound surface modifiers, have proven to be quite effective in the elimination of any protein–capillary interactions. Using a capillary permanently coated with poly(vinyl alcohol) (PVA) and another which was covalently bonded with linear polyacrylamide (LPA), we employed the pressure-driven propagation method for each of the five representative proteins. It is clear from Figures S1–S5 in the Supporting Information that PVA considerably reduced protein adsorption for conalbumin, cytochrome *c*, thrombin, and lysozyme. Lysozyme still demonstrated a clear interaction with the PVA surface; however, there is a notable improvement from both the uncoated and dynamically coated capillaries. The capillary coated with LPA did not perform as well as the PVA-coated capillary or the capillary coated with CElixir dynamic modifier, though it was an improvement to the bare-silica capillary. Covalently bound polyacrylamide is typically quite efficient at preventing protein adsorption in CE. However, the run buffer used in all of the described experiments had a pH value of 8.2, which may have prompted LPA hydrolysis and reduced the coating's effectiveness.<sup>32</sup>

To rank each coating, the peak shape, width, and intensity were first analyzed. If no clear visual distinction can be made, then the amount of protein adsorbed was estimated by integrating the peak areas and then comparing the values obtained between the 10 and 40 cm propagations for a given protein and coating. In the case of AGP, both the uncoated capillary and capillary coated with CElixir were 100% effective in preventing protein adsorption, and thus, both coatings were given equal rankings.

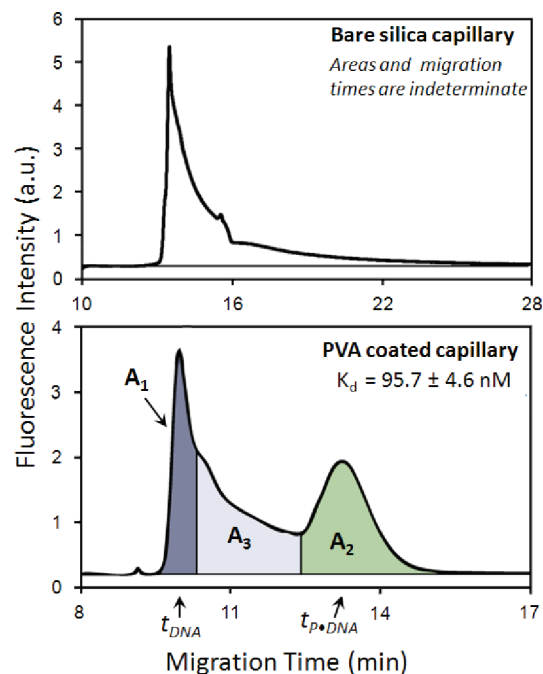


**Figure 4.** NECEEM electropherograms produced using the thrombin–aptamer binding system using an uncoated capillary (top panel) and PVA-coated capillary (lower panel). The equilibrium mixtures consisted of 455 nM thrombin and 91 nM TBA and were separated using normal polarity in the uncoated capillary and reverse polarity with the PVA coating. The areas corresponding to free aptamer ( $A_1$ ), aptamer dissociated from the complex ( $A_3$ ), and intact complex ( $A_2$ ) are identified in the electropherogram produced using the PVA-coated capillary. The uncoated capillary could not be analyzed as the areas are poorly defined.

Due to its anionic properties, AGP ( $pI = 2.8–3.8$ ) demonstrated a minimal interaction with the fused-silica surface, and thus, an uncoated capillary suffices for its CE analysis. For conalbumin, both PVA and CElixir coatings produced similar results in terms of protein loss (each a significant improvement from the uncoated capillary) and were also given equal rankings. The results shown in Table 1 suggest that different proteins respond differently to the same coating, and there may be no simple and universal solution to prevent protein adsorption at neutral pH. Proteins themselves vary in their overall charge and structure and each will experience a unique interaction with different wall chemistries.

To further verify the advantages of this technique, and demonstrate how the protein's temporal propagation pattern can facilitate KCE-based analysis, we performed a set of separation-based affinity experiments using the thrombin–aptamer binding pair as a model. These experiments are termed nonequilibrium capillary electrophoresis of equilibrium mixtures (NECEEM) and are commonly used to measure the kinetic and equilibrium constants of protein–aptamer interactions.<sup>2,33</sup> Briefly, a mixture containing a fluorescently labeled aptamer is incubated with the target protein to establish equilibrium between the protein–aptamer complex and its unbound counterparts. A sample plug containing this equilibrium mixture is then introduced into the capillary and subjected to electrophoresis. As the protein, aptamer, and protein–aptamer complex separate, equilibrium is perturbed, and the complex starts to continuously dissociate. The kinetic and equilibrium parameters are obtained by integrating the areas which correspond to the free aptamer ( $A_1$ ), aptamer–protein complex ( $A_2$ ),

and aptamer that has dissociated from the complex during separation ( $A_3$ ). We performed consecutive NECEEM experiments using two different capillary surfaces, one demonstrating strong adsorption toward thrombin and the other having only a negligible affinity. As indicated in Table 1, the PVA coating ranked highest in terms of its antiadhesive properties while the uncoated capillary ranked lowest with respect to the thrombin sample; therefore, these two capillary surfaces were chosen for NECEEM analysis.

When using the uncoated capillary and performing separation with the cathode at the capillary outlet, we would expect the complex to migrate faster than the free aptamer and, under ideal conditions, reach the detector first. However, as seen from Figure 4, the areas of free aptamer and aptamer dissociated from the complex are indefinable, and no clear complex peak was observed. The experiment was then repeated using the PVA-coated capillary, with the anode at the outlet due to the absence of an EOF. The acquired results were precisely as expected, with the aptamer peak reaching the detector first, followed by the aptamer dissociated from the complex and finally the intact complex. The areas were easily integratable and enabled accurate kinetic analysis of the thrombin–aptamer interaction. These results confirm that the pressure-driven protein propagation can be used to improve the quality of KCE analyses that involve adsorptive protein samples.

We propose this simple and fast method for screening a series of coatings to help select the optimal conditions for the KCE methods involving proteins. This method promises to help expand the number of biomolecular interactions studied by KCE and assist in KCE-based aptamer selection.

## CONCLUDING REMARKS

Here we demonstrate a simple and universal method for screening various capillary coatings for protein analysis in KCE. We proved that this approach can be readily used to rank the antiadhesive properties of different capillary surfaces for important protein samples. We illustrate the difficulties associated with the KCE studies involving adsorptive proteins and propose a method that will improve the analysis by selecting the appropriate capillary coating. This technique will undoubtedly assist in diversifying the number of protein–ligand interactions studied by KCE methods and improve the efficiency of KCE-based aptamer selection.

## MATERIALS AND METHODS

**Materials.** Chromeo P503 fluorescent labeling pyrylium dye was purchased from Active Motif (Burlington, ON, Canada). The HPLC-purified thrombin-binding aptamer (5'-Alexa488-CGG TTG GTG TGG TTG GAA AAA AAA AAA AAA AAA AAA A-3') was obtained from Integrated DNA Technologies (Coralville, IA), dissolved to a concentration of 50  $\mu\text{M}$  in 10 mM Tris–HCl (pH 7.5), and stored at  $-20^\circ\text{C}$  until use.

Lyophilized protein samples ( $\alpha_1$  acid glycoprotein, conalbumin, cytochrome *c*, and lysozyme) and all other chemicals were purchased from Sigma-Aldrich (Oakville, ON, Canada). Solutions were made with deionized water and passed through a 0.22  $\mu\text{m}$  filter by suction (Millipore, Nepean, ON, Canada). Uncoated fused-silica capillaries with an inner diameter of 75  $\mu\text{m}$  (375  $\mu\text{m}$  outer diameter) were purchased from Polymicro (Phoenix, AZ). Neutral capillaries covalently bonded with linear

polyacrylamide (75  $\mu\text{m}$  i.d., 365  $\mu\text{m}$  o.d.) and the CELixir dynamic coating system consisting of initiator and accelerator (pH 8.2) solutions were purchased from MicroSolv Technology Corp. (Eatontown, NJ).

**Instrumentation.** All experiments were performed using a P/ACE MDQ capillary electrophoresis instrument (Beckman-Coulter, Fullerton, CA) equipped with either a laser-induced fluorescence (LIF) or photodiode array (PDA) detection system. For pressure-driven propagation experiments a continuous 488 nm solid-state laser line was used to excite the fluorescence of both the DNA and protein samples. Due to the considerable variation in their fluorescence emission spectra, a two-channel detector was employed to effectively separate the DNA and protein fluorescence into two discrete channels. Band-pass filters specific for 520 and 610 nm were used to isolate fluorescence signals from Alexa488-labeled DNA and Chromeo P503-labeled proteins, respectively.

**Protein Labeling.** Lyophilized proteins (AGP, cobalbumin, cytochrome *c*, and lysozyme) were dissolved in a 0.1 M solution of  $\text{NaHCO}_3$  (pH 8.2) to a concentration of 4 mg/mL. A working solution of Chromeo P503 was added to each protein sample in a 1:100 volume ratio of dye to protein. Thrombin was labeled by diluting the protein stock in a Chromeo mixture, containing 1  $\mu\text{L}$  of Chromeo P503 and 100  $\mu\text{L}$  of 0.1 M  $\text{NaHCO}_3$  (pH 8.3), to obtain a final thrombin concentration of 48  $\mu\text{M}$ . All labeling reactions were left to incubate overnight at  $4^\circ\text{C}$  to complete the conjugation. Protein solutions were then aliquoted and stored at  $-20^\circ\text{C}$  until use. All samples were then diluted in 0.1 M  $\text{NaHCO}_3$  (pH 8.3) to obtain the final concentrations.

**Poly(vinyl alcohol) Coating.** PVA (5%, w/v) was prepared by dissolving the polymer in boiling deionized water. An uncoated fused-silica capillary was sequentially flushed with 0.1 M NaOH and deionized water for 1 h under a 12 psi flow of nitrogen gas. The pretreated capillary was then flushed with the PVA solution for 10 min at 15 psi and emptied using a 10 psi gas flow for 10 min. PVA was immobilized on the capillary surface by drying overnight in an oven set at  $140^\circ\text{C}$  and continuously flushed with a low pressure of nitrogen.<sup>34</sup> The detection window was made using a fuming solution of  $\text{H}_2\text{SO}_4$  to preserve the integrity of the coating at the detection site.

**Experimental Conditions.** All experiments were performed using a 50 cm capillary (40 cm to detection window). Bare silica capillaries were pretreated by rinsing with methanol for 10 min at 20 psi. Prior to each run, the uncoated capillary was rinsed with RNase AWAY solution using 20 psi for 5 min followed by a sequential rinse with 0.1 M HCl, 0.1 M NaOH, doubly distilled water ( $\text{ddH}_2\text{O}$ ), and 50 mM Tris acetate (pH 8.2) at 20 psi for 2 min. Dynamically modified capillaries were prepared using the commercial CELixir double-layer system. The capillary was preconditioned by first rinsing with 0.1 M NaOH for 5 min followed by deionized water for 2 min, each at a pressure of 29 psi. The coating was administered by rinsing the capillary with the initiator and accelerator (pH 8.2) solutions at 20 psi for 1 and 2 min, respectively. This coating procedure was repeated prior to each run. Before each experiment, the permanently coated PVA capillary was rinsed with  $\text{ddH}_2\text{O}$  and 50 mM Tris acetate (pH 8.2), each at 20 psi for 8 min.

All samples were introduced into the capillary by applying a 6 s pressure pulse of 0.5 psi. Pressure-driven propagation analyses were carried out using the 50 mM Tris acetate (pH 8.2) run buffer for both the uncoated and PVA-coated capillaries, while the CELixir accelerator solution (pH 8.2) was used in the

dynamically modified capillary. A 0.5 psi forward pressure was applied for the 40 cm propagation, and a reverse pressure of the same magnitude was used for the 10 cm propagation experiments.

UV absorbance experiments were performed using an uncoated fused-silica capillary. Separation was carried out at 300 V/cm with 50 mM Tris acetate (pH 8.2) as the background electrolyte. Dimethyl sulfoxide (DMSO; 0.2%) was used as a neutral marker to measure the protein influence on the EOF. The EOF mobility values shown in Figure 1 were calculated using the following equation:

$$\mu_{\text{EOF}} = \frac{L_t L_d}{U t_m}$$

where  $U$  is the applied voltage,  $t_m$  is the migration time to the detector,  $L_t$  is the total capillary length, and  $L_d$  is the distance from the capillary inlet to the detector.

#### NECEEM Analysis of the Thrombin–Aptamer Interaction.

A 1  $\mu\text{M}$  solution of the thrombin-binding aptamer (TBA) was heated to 95 °C for 1 min using a thermal cycler (Eppendorf, Hamberg, Germany) and gradually cooled to 25 °C at a rate of 0.5 °C/s to promote proper aptamer folding.

An equilibrium mixture consisting of 455 nM thrombin and 91 nM TBA was prepared in a 20 mM Tris acetate (pH 8.2) buffer containing 5 mM KCl and 1 mM  $\text{MgCl}_2$ . The mixture was separated using 10 kV for the first 5 min followed by an increase to 20 kV in the uncoated capillary to avoid sample overheating. When using the PVA-coated capillary, the same voltages were applied; however, the electric field polarity was reversed. The equilibrium dissociation constants were calculated using the following equation:

$$K_d = \frac{[P]_0 \{1 + A_1/(A_2 + A_3)\} - [\text{DNA}]_0}{1 + (A_2 + A_3)/A_1}$$

where  $[P]_0$  and  $[\text{DNA}]_0$  are the initial protein and aptamer concentrations, respectively, and  $A_1$ ,  $A_2$ , and  $A_3$  correspond to the integrated areas of free aptamer, complex, and aptamer dissociated from the complex, respectively. The areas were corrected for differences in the propagation velocities for free and bound aptamers.

## ■ ASSOCIATED CONTENT

**S Supporting Information.** Additional information as noted in text. This material is available free of charge via the Internet at <http://pubs.acs.org>.

## ■ AUTHOR INFORMATION

### Corresponding Author

\*E-mail: [skrylov@yorku.ca](mailto:skrylov@yorku.ca).

## ■ ACKNOWLEDGMENT

This work was funded by the Natural Sciences and Engineering Research Council of Canada.

## ■ REFERENCES

- (1) Petrov, A.; Okhonin, V.; Berezovski, M.; Krylov, S. N. *J. Am. Chem. Soc.* **2005**, *127*, 17104–17110.
- (2) Berezovski, M.; Krylov, S. N. *J. Am. Chem. Soc.* **2002**, *124*, 13674–13675.
- (3) Okhonin, V.; Berezovski, M.; Krylov, S. N. *J. Am. Chem. Soc.* **2004**, *126*, 7166–7167.

- (4) Krylov, S. N. *J. Biomol. Screening* **2006**, *11*, 115–122.
- (5) Østergaard, J.; Heegaard, N. H. H. *Electrophoresis* **2006**, *27*, 2590–2608.
- (6) Okhonin, V.; Petrov, A.; Berezovski, M.; Krylov, S. N. *Anal. Chem.* **2006**, *78*, 4803–4810.
- (7) Krylov, S. N. *Electrophoresis* **2007**, *28*, 69–88.
- (8) Okhonin, V.; Berezovski, M.; Krylov, S. N. *J. Am. Chem. Soc.* **2010**, *132*, 7062–7068.
- (9) Schure, M. R.; Lenhoff, A. M. *Anal. Chem.* **1993**, *65*, 3024–3037.
- (10) Gaš, B.; Štědrý, M.; Kennedler, E. *Electrophoresis* **1997**, *18*, 2123–2133.
- (11) Towns, J. K.; Regnier, F. E. *Anal. Chem.* **1992**, *64*, 2473–2478.
- (12) Bello, M. S.; Capelli, L.; Righetti, P. G. *J. Chromatogr., A* **1994**, *684*, 311–322.
- (13) McCormick, R. M. *Anal. Chem.* **1988**, *60*, 2322–2328.
- (14) Lauer, H. H.; McManigill, D. *Anal. Chem.* **1986**, *58*, 166–170.
- (15) Towns, J. K.; Regnier, F. E. *Anal. Chem.* **1992**, *63*, 1132–1138.
- (16) Regnier, F. E. *Science* **1987**, *238*, 319–323.
- (17) Yao, Y. L.; Khoo, K. S.; Chung, M. C. M.; Li, J. *J. Chromatogr.* **1994**, *680*, 431–435.
- (18) Wiktorowicz, J. E.; Colburn, J. C. *Electrophoresis* **1990**, *11*, 769–773.
- (19) Dong, M. Q.; Oda, R. P.; Strausbauch, M. A.; Wettstein, P. J.; Landers, J. P.; Miller, L. J. *Electrophoresis* **1997**, *18*, 1767–1774.
- (20) Legaz, M. E.; Pedrosa, M. M. *J. Chromatogr., A* **1996**, *719*, 159–170.
- (21) Córdova, E.; Gao, J.; Whitesides, G. M. *Anal. Chem.* **1997**, *69*, 1370–1379.
- (22) Lucy, C. A.; MacDonald, A. M.; Gulcev, M. D. *J. Chromatogr., A* **2008**, *1184*, 81–105.
- (23) (a) Verzola, B.; Gelfi, C.; Righetti, G. *J. Chromatogr., A* **2000**, *868*, 85–99. (b) Verzola, B.; Gelfi, C.; Righetti, G. *J. Chromatogr., A* **2000**, *874*, 293–303. (c) Castelletti, L.; Verzola, B.; Gelfi, C.; Stoyanov, A.; Righetti, G. *J. Chromatogr., A* **2000**, *894*, 281–289.
- (24) Tran, N. T.; Taverna, M.; Miccoli, L.; Angulo, J. F. *Electrophoresis* **2005**, *26*, 3105–3112.
- (25) Ramsay, L. M.; Dickerson, J. A.; Dada, O.; Dovichi, N. J. *Anal. Chem.* **2009**, *81*, 1741–1746.
- (26) Ramsay, L. M.; Dickerson, J. A.; Dovichi, N. J. *Electrophoresis* **2009**, *30*, 297–302.
- (27) de Jong, S.; Krylov, S. N. *Anal. Chem.* **2011**, *83*, 6330–6335.
- (28) Okhonin, V.; Liu, X.; Krylov, S. N. *Anal. Chem.* **2005**, *77*, 5925–5929.
- (29) Righetti, P. G.; Gelfi, C.; Verzola, B.; Castelletti, L. *Electrophoresis* **2001**, *22*, 603–611.
- (30) Chevigné, R.; Louis, P. U.S. Patent 5 611 903, 1997.
- (31) Boone, C. M.; Jonkers, E. Z.; Franke, J. P.; de Zeeuw, R. A.; Ensing, K. *J. Chromatogr., A* **2001**, *927*, 203–210.
- (32) Nakatani, M.; Shibukawa, A.; Nakagawa, T. *Electrophoresis* **1995**, *16*, 1451–1456.
- (33) Berezovski, M.; Nutiu, R.; Li, Y.; Krylov, S. N. *Anal. Chem.* **2003**, *75*, 1382–1386.
- (34) Belder, D.; Deege, A.; Husmann, H.; Kohler, F.; Ludwig, M. *Electrophoresis* **2001**, *22*, 3813–3818.

## Supporting Information

### Pressure-Based Approach for the Analysis of Protein Adsorption in Capillary Electrophoresis

Stephanie de Jong and Sergey N. Krylov

*Department of Chemistry and Centre for Research on Biomolecular Interactions, York University, Toronto, Ontario M3J 1P3, Canada*

#### Capillary surface chemistry influence on the temporal propagation pattern of several proteins

Protein adsorption was characterized using the dual-detection pressure-driven propagation method as described in the main text. Representative proteins, each with unique surface properties and charge, were chosen as models to illustrate the applicability of this method. Chromeo labeled proteins were diluted in a 0.1 M NaHCO<sub>3</sub> (pH 8.2) buffer to obtain the following concentrations: 9.8 μM α<sub>1</sub>- acid glycoprotein, 5.3 μM conalbumin, 10.1 μM thrombin, 171 μM cytochrome C, and 137 μM lysozyme. 30 nL of the sample was injected into the capillary inlet and carried 40 cm to the detector using a low forward pressure of 0.5 psi to guarantee adequate diffusion between the sample and buffer plugs. The 10 cm propagation was performed using the same capillary however, the sample was injected from the outlet end and each pressure was applied in the reversed direction. The experimental analysis of protein adsorption was performed using capillaries with four different surface chemistries: (i) a bare silica capillary, (ii) a capillary coated with the CELixir dynamic modification system, (iii) a capillary with a permanently adsorbed poly(vinyl) alcohol (PVA) surface and (iv) a capillary with a covalently bonded linear polyacrylamide (LPA) surface. For the uncoated, PVA-coated, and LPA-coated capillaries we had employed a run buffer of 50 mM Tris acetate (pH 8.2). The dynamically coated capillary used the commercially available CELixir accelerator solution at pH 8.2 as the run buffer. All experiments were performed in triplicates with less than 15% standard deviation in the integrated peak areas to ensure reproducibility. Protein adsorption was determined by comparing peak height, width and symmetry of each pressure propagation profile. In addition, the differences in peak area between the 10-cm and 40-cm propagation were used to assess the degree of protein adsorption by calculating the amount of protein loss during the 30-cm migration. Representative results for each coating protein are shown in Figs. S1, S2, S3, S4, and S5 below.

# AGP Adsorption

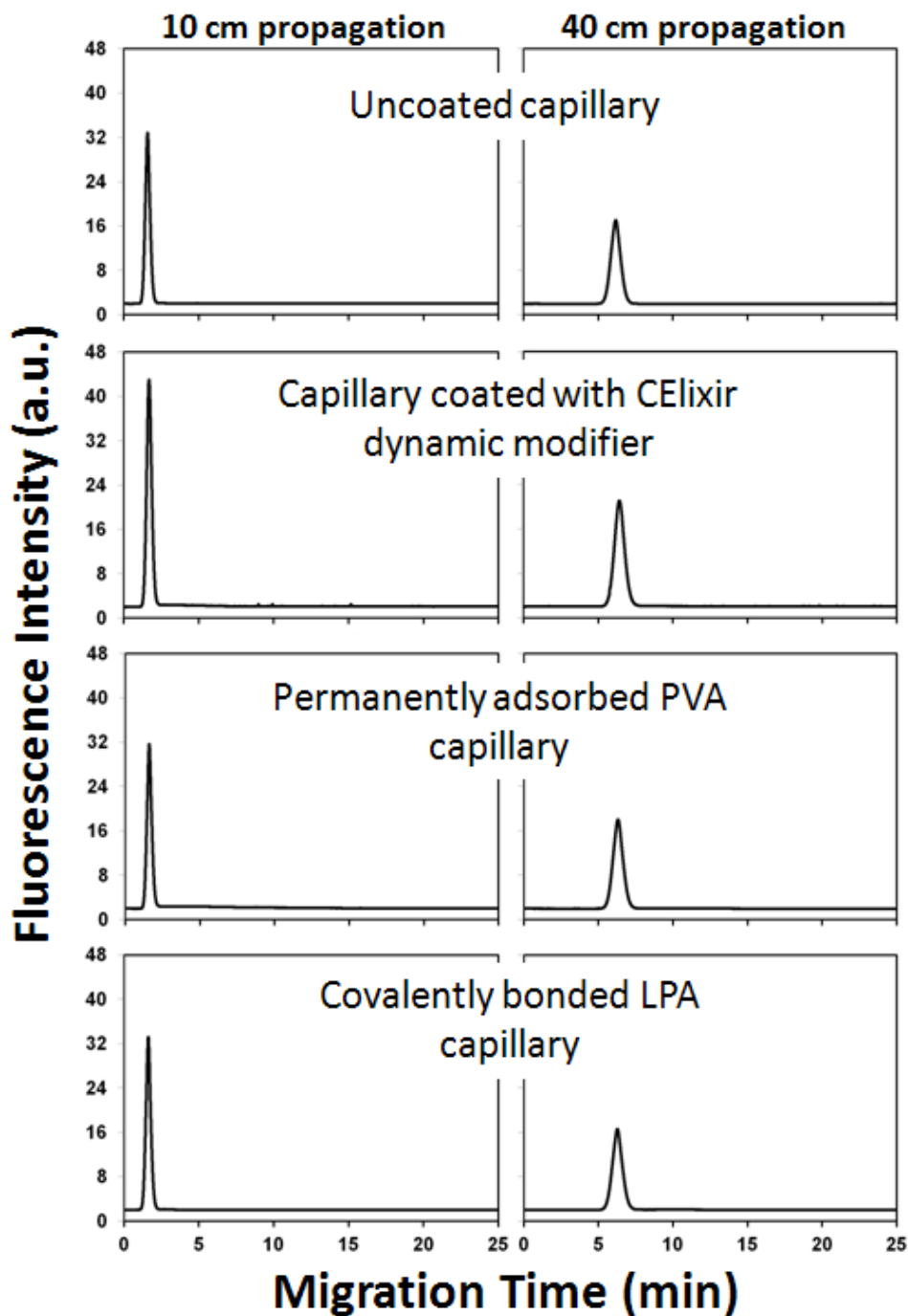


**Figure S1.** Temporal propagation patterns of 9.8  $\mu\text{M}$  Chromeo-labeled AGP after 10-cm and 40-cm pressure-driven propagations using an uncoated capillary, a capillary coated with CELixir dynamic modifier, a capillary with a permanently adsorbed PVA coating and a capillary covalently bonded with LPA.



# Conalbumin Adsorption

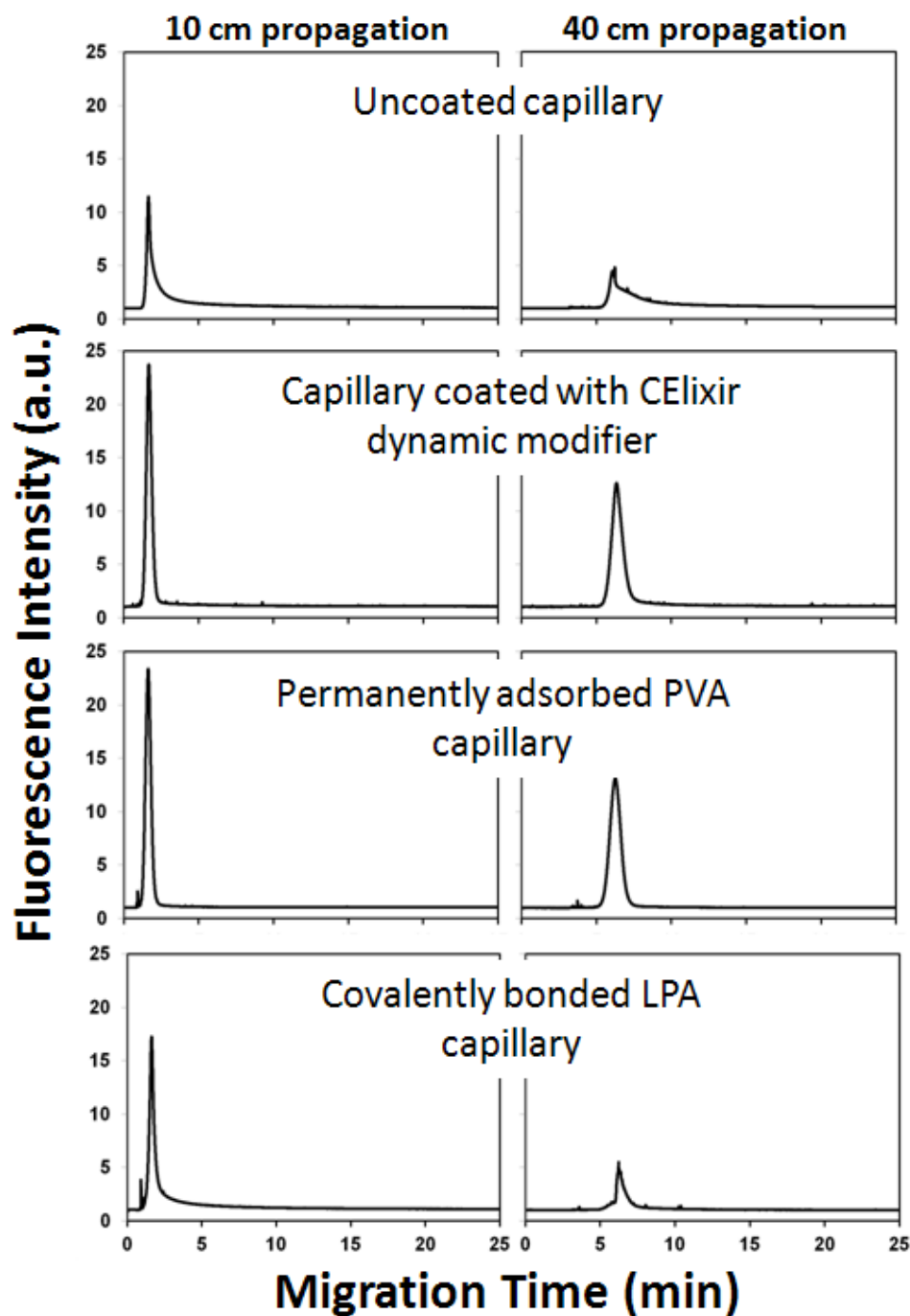


**Figure S2.** Temporal propagation patterns of 5.3  $\mu\text{M}$  Chromeo-labeled conalbumin after 10-cm and 40-cm pressure-driven propagations using an uncoated capillary, a capillary coated with CELixir dynamic modifier, a capillary with a permanently adsorbed PVA coating and a capillary covalently bonded with LPA.

# Thrombin Adsorption

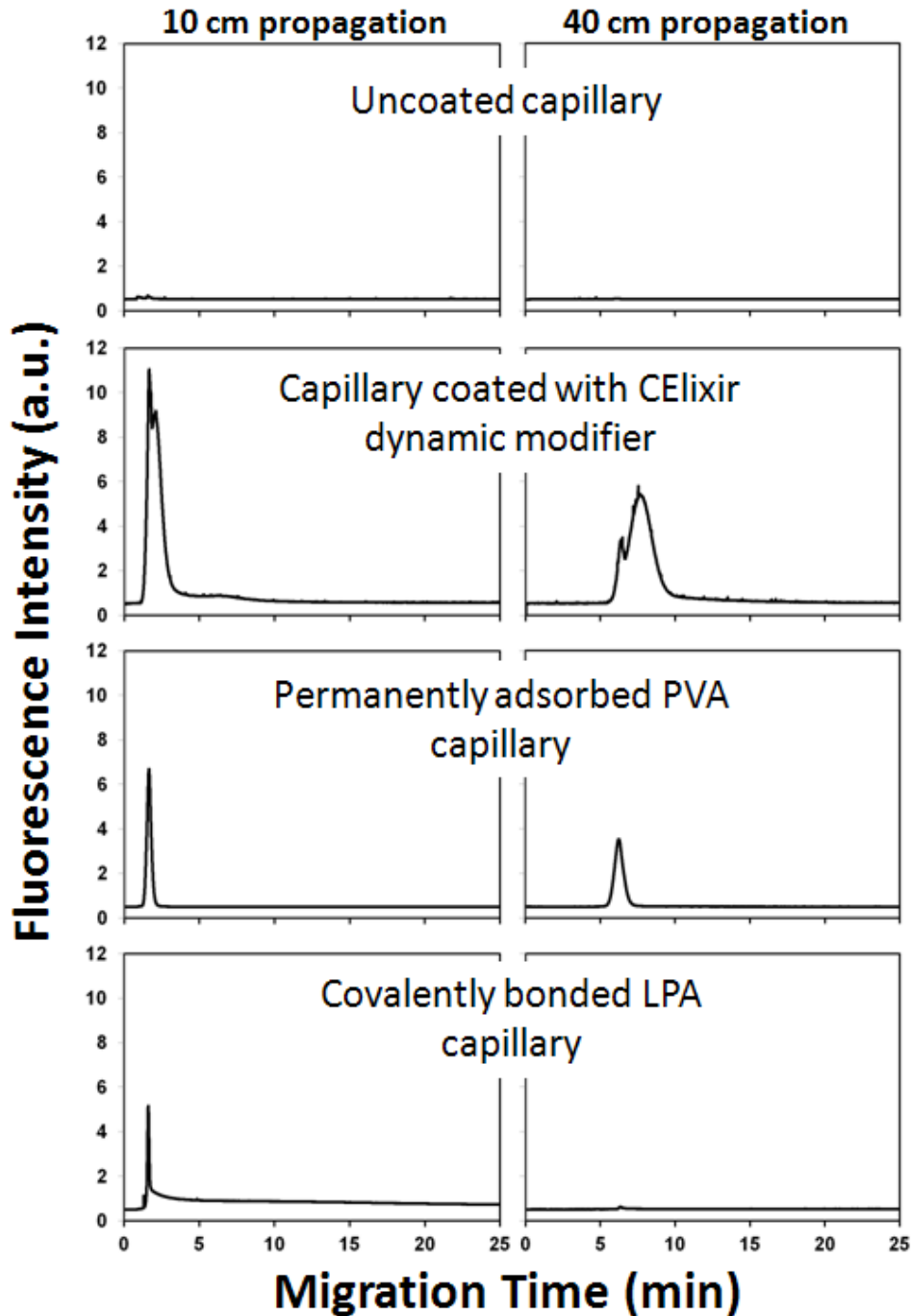


**Figure S3.** Temporal propagation patterns of 10.1  $\mu\text{M}$  Chromeo-labeled thrombin after 10-cm and 40-cm pressure-driven propagations using an uncoated capillary, a capillary coated with CELixir dynamic modifier, a capillary with a permanently adsorbed PVA coating and a capillary covalently bonded with LPA.

# Cytochrome C Adsorption

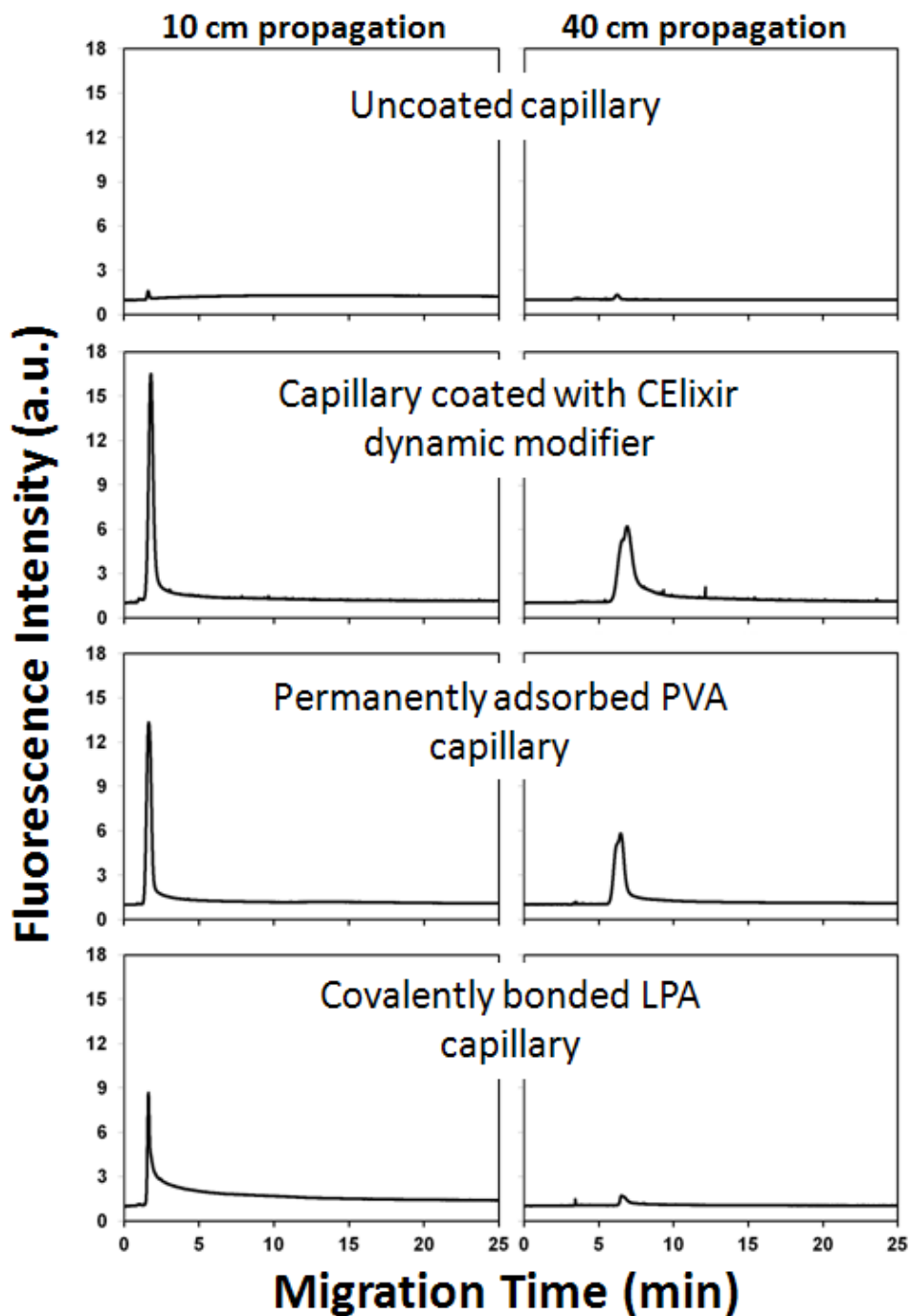


**Figure S4.** Temporal propagation patterns of  $171\mu\text{M}$  Chromeo-labeled cytochrome C after 10-cm and 40-cm pressure-driven propagations using an uncoated capillary, a capillary coated with CELixir dynamic modifier, a capillary with a permanently adsorbed PVA coating and a capillary covalently bonded with LPA.

# Lysozyme Adsorption

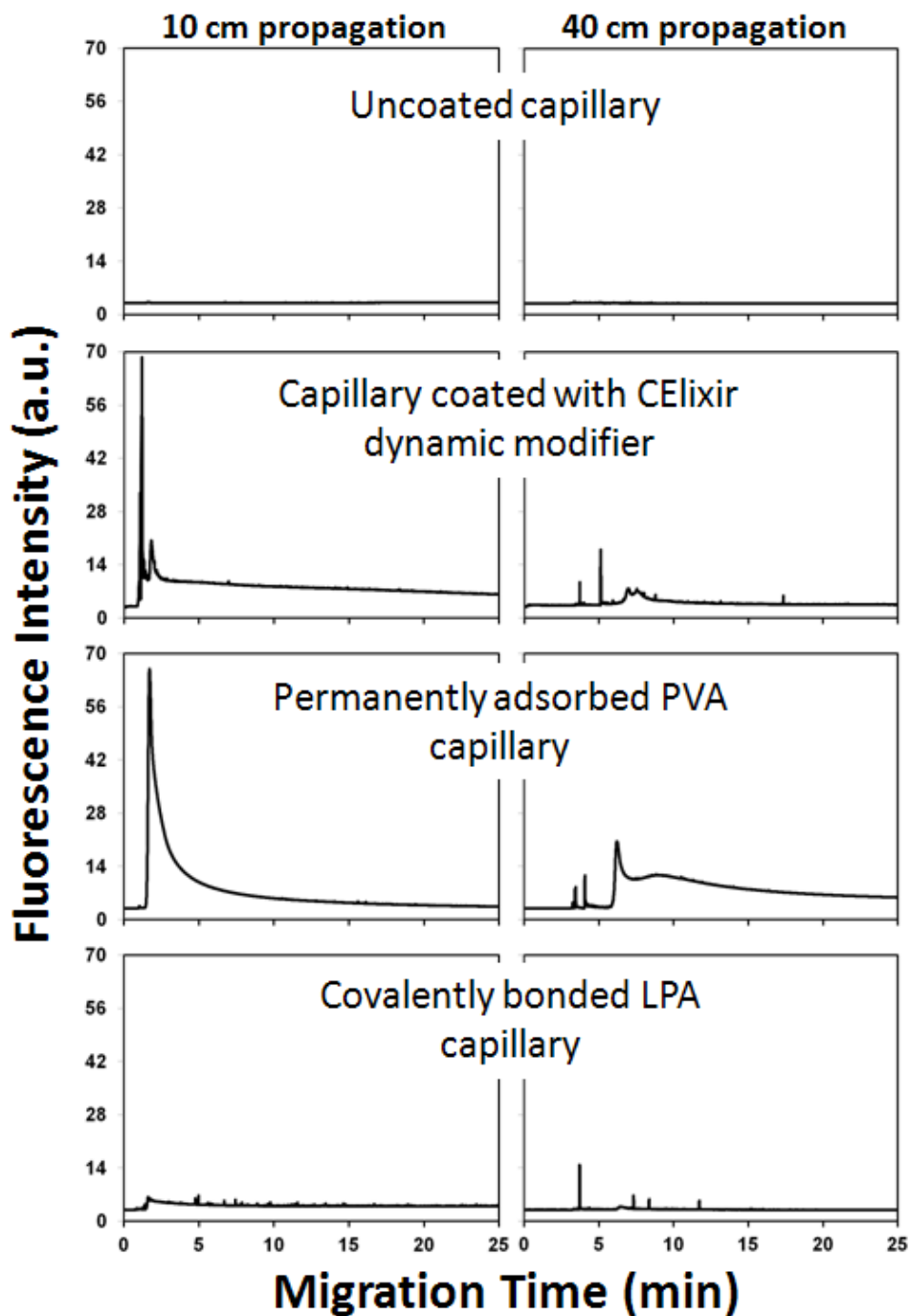


**Figure S5.** Temporal propagation patterns of 137  $\mu\text{M}$  Chromeo-labeled lysozyme after 10-cm and 40-cm pressure-driven propagations using an uncoated capillary, a capillary coated with CELixir dynamic modifier, a capillary with a permanently adsorbed PVA coating and a capillary covalently bonded with LPA.